A COUPLED BUILDING VENTILATION AND THERMAL MODEL INCORPORATING PASSIVE AIRFLOW COMPONENTS

Alemu T Alemu, Wasim Saman, and Martin Belusko
Barbara Hardy Institute, University of South Australia, Adelaide, Australia

ABSTRACT

This paper investigates the inclusion of passive airflow components such as solar chimney, and wind induced earth air tunnel into a coupled multi-zone ventilation and thermal model. Existing commercial coupled multi-zone ventilation and thermal modelling software do not include passive airflow components, which need a simultaneous prediction of temperature and airflow rate in the components. The present model is compared with the coupled COMIS-TRNSYS software for lightweight buildings with large openings and both the thermal and airflow prediction match with good accuracy. The predictions of individual passive airflow components are validated with available published analytical and experimental findings.

INTRODUCTION

Effective integration of passive features into the building design can significantly minimise the air-conditioning demand in buildings while maintaining thermal comfort(Santamouris 2007). Passive features are components, which can be integrated as part of the building at the design stage to induce ventilation and cooling, and therefore replace or reduce the need for a mechanical cooling and ventilation system. These elements may include solar chimneys, wind induced earth air tunnels (EAT) and passive evaporative cooling towers. Due to variable responses of passive systems, the use of a combination of these features has the potential to significantly increase the ability to meet the cooling energy demanded to achieve thermal comfort in a building. Commercial coupled multi-zone airflow and thermal modelling software such as COMIS-TRNSYS, CONTAM-TRNSYS or TRNFLOW are well known for their capability to assess natural ventilation (Chen 2009) . Unfortunately, passive elements such as solar chimney, and wind driven earth EAT cannot be modelled with the available air flow components as the flow through these elements is mainly dependent on buoyancy in each component and building pressure distribution. For example a chimney may be represented as a duct element in both COMIS and CONTAM, however, in this assumption the chimney can only act as a stack, whereas in solar chimney the main driving force is the buoyancy due to the absorbed solar radiation in solar chimney channel. The model hence needs to incorporate a simultaneous prediction of temperature and airflow rate in the solar chimney. Apart from the multi-zone modelling software, most available simplified models of passive systems (Ong & Chow 2003; Bahadori, Mazidi & Dehghani 2008; Bassiouny & Koura 2008) do not consider the building pressure distribution. As a result, these models are not applicable when multiple openings, multi-zone and infiltration require consideration. Limited research has been conducted on modelling of combined passive ventilation systems (Bansal, Mathur & Bhandari 1994; Maerefat & Haghighi 2010). However, these research are based on a single zone with two openings without due consideration to building pressure variation. Furthermore, the models do not consider wind effects and flow reversal. Using CFD is an option for studying such systems and it is commonly used as a design check. However to conduct a design and optimisation study to maximise thermal comfort over a year, CFD is not a feasible solution (Ohba & Lun 2010). The objective of this paper is to develop a mathematical model to incorporate passive features into a multi-zone ventilation and thermal building model.

MATHEMATICAL MODEL

Figure 1, presents the structure of the mathematical model consisting of a multi zone building ventilation model with integrated passive cooling features. The model applies quasi steady state for each simulation hour. A separate fluid dynamic and thermal model was developed for each individual passive element.

In these components the temperature and airflow rate are predicted iteratively taking into account the zone pressure, and pressure drop in the components. The solution is iteratively found such that the percentage error of air mass flow rate ($error_{\dot{m}}$) and the temperature ($error_T$) in the components is less than minimum error allowable (ε_m & ε_T). The mass flow rate $\dot{m}$, the partial derivative of the flow rate with respect to the zone pressure $\frac{\partial \dot{m}}{\partial P_i}$, and the exit temperature (T) from the components are then fed to the multi-zone ventilation model. The zone pressure (P_i) is updated by the ventilation model and is given

as input into the components until the solution satisfies the maximum residual of mass balance of each zone $\max|error_{t\dot{m}_i}|$ and maximum error in zones' pressures $\max|error_{Pi}|$ are less than allowable limits ($\varepsilon_{t\dot{m}_i}$ & ε_{Pi}). The mass flow rate for all openings in each zone and the temperature output from the components will be input to the building thermal model and the temperature of each zone is calculated and fed back to the ventilation and components model. The solution for each time step is converged when the maximum error in zones temperatures $error_{Ti}$ is less than allowable limitε_{T_i}.

Multi zone ventilation model

In the multi-zone ventilation model developed, a building is idealized as a system of zones linked together by discrete airflow paths. Zones are represented by nodes. A hydrostatic condition is assumed in zones and the flow rate in each link is defined as a function of zone pressure, which results in a system of non linear equations, defined by the mass conservation for each zone. The equations are solved numerically to predict zone pressures, which are back substituted in flow equations to predict airflow rate at each link.

A technique used by Zhengen and Zhendong (2009) is modified to add wind and buoyancy driven flow components in addition to large openings, crack and infiltration. The detailed equations used for large openings and cracks are presented in (Zhengen & Zhendong 2009).

The present model includes special airflow components, which need simultaneous prediction of temperature and airflow rate in the components. This strategy allows passive features such as solar chimney, and wind induced earth-air tunnel to be easily integrated into coupled multi-zone ventilation and thermal models. For openings connected to these passive features, a one-way flow through large opening is assumed. Using dynamic pressure head at the inlet of the flow components as a reference, the mass-pressure relationship can be expressed as

$$\dot{m} = 2^n C_{syst}\, A_{in} {\rho_{in}}^{1-n} |\Delta p_{av}|^n sign(\Delta p_{av}) \qquad (1)$$

Where $\dot{m}$ is the mass flow rate through opening connected to the component, C_{syst} is the system flow coefficient, n is pressure exponent and generally n=0.5 for large openings. A_{in} inlet opening area; ρ_{in} density of air inlet to the component, Δp_{av} is the available pressure and $sign(\Delta p_{av})$ is the indicator of sign of the available pressure. If Δp_{av} is positive, the air is flowing into the zone. i.e negative $\dot{m}$ indicates the airflow is from the zone into the component.

The mass conservation for each zone $f_i(p_i, p_j)$ results in a system of non linear equations equal to the number of zones evaluated.

$$f_i(P_i, P_j) = \sum_{j=1}^{N_i} \dot{m}_{j,i} = 0 \qquad \text{i=1,2,...,N} \qquad (2)$$

Where N, N_i, and $\dot{m}_{j,i}$ are number of zones, number of openings in zone i and net mass flow rate through an opening j respectively. P_i, and P_j are zone i's and connected zone j's static pressure respectively.

The equations are simultaneously solved using globally convergent Newton's Method. Details of the solution procedure can be obtained in Dennis & Schnabel (1996). This method is generally convergent for a wide range of initial pressure guesses.

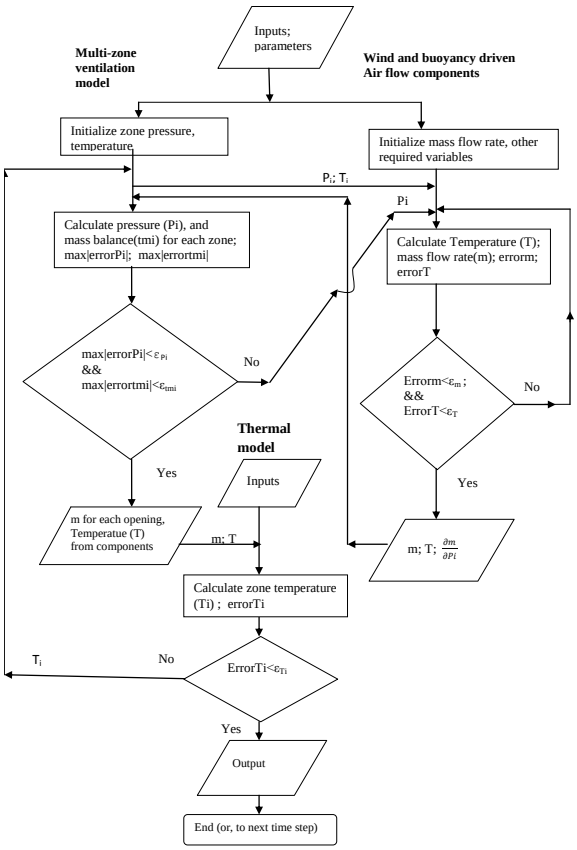

Figure 1 A zone connected to roof mounted solar chimney; wall mounted solar chimney and wind driven earth air tunnel.

Mass flow rate and temperature prediction in solar chimney

A number of mathematical models have been completed for predicting the mass flow rate in a solar chimney (Ong & Chow 2003; Bassiouny & Koura 2008).The models principally assume no pressure difference across the chimney except the stack effect and therefore do not consider the pressure distribution of the building, resulting in an incorrect determination of the flow in the chimney. The pressure head in the chimney is always positive as long as the mean air temperature in the chimney is greater than the room temperature. These models assume flow is always induced in the chimney regardless of the pressure drops encountered in the

system and the building pressure distribution and, as a result, they fail to predict reverse flow. By ignoring the building pressure distribution, the models will not determine the correct flow in case of multi-openings in either the connected zone, multi-zone building and in hybrid mode. In the present paper, the zone pressure and pressure drops are considered in the mass flow rate relationship.

The available pressure Δp_{av} between the inlet and outlet of roof mounted solar chimney (figure 2) can be derived using Bernoulli's principle. The relationship assumes a constant density in the channel equal to the average density, constant zone density, and applies hydrostatic pressure difference in the zone with elevation.

$$\Delta p_{av} = \frac{\rho_a C p U^2}{2} + \rho_a g\left(H_{ref} - \left(f_i + R_i + L\cos(\theta)\right)\right) - \left(p_i - H_i g \rho_i - \rho_{cav} g L\cos(\theta)\right) \quad (3)$$

Where ρ_a and c_p are external air density and wind pressure coefficient at solar chimney outlet

U is the wind speed at the building reference height

ρ_i is zone air density

ρ_{cav} is average air density in the solar chimney

g is the gravitational acceleration

P_i is static pressure at the zone's mid height (H_i) with reference to atmospheric pressure at building reference height H_{ref}.

f_i is the elevation of the zone's floor from the ground

R_i is the ceiling height of the zone

L is length of the solar chimney

θ inclination angle of the solar chimney from vertical

Similarly, Δp_{av} for a wall mounted solar chimney (figure 2) can be derived as

$$\Delta p_{av} = \frac{\rho_a C p U^2}{2} + \rho_a g\left(H_{ref} - (f_i + H_{in} + L)\right) - (P_i + g\rho_i(H_i - H_{in}) - \rho_{cav} g L) \quad (4)$$

Where H_{in} *is* inlet opening's height of the solar chimney from the zone's floor.

The mass flow rate in the solar chimney can be evaluated as

$\dot{m} = 2^n C_{syst}\, A_{in}{\rho_{in}}^{1-n}|\Delta p_{av}|^n sign(\Delta p_{av})$,

Where:

$$C_{syst} = \frac{1}{\left(1 + {A_{in}^2\rho_{in}}/{A_{out}^2\rho_{out}} + \xi_{in} + \xi_{lfr} + \xi_{out} + \xi_{ldirout}\right)^{0.5}} \quad (5)$$

A_{in} *and* A_{out} are inlet and outlet area of the solar chimney

Loss coefficients due to friction ξ_{lfr} and local losses at inlet ξ_{in}, outlet ξ_{out}, and change in direction $\xi_{ldirout}$ are evaluated with reference to the dynamic pressure at the inlet $\dot{m}/(2A_{in}^2\rho_{in})$ and presented in detail in Syrios & Hunt (2004).

For implementation into the Newton's method, the Jacobean coefficient with respect to the connected zone pressure P_i can be calculated as

$$\frac{\partial \dot{m}}{\partial p_i} = -n2^n C_{syst}\, A_{in}{\rho_{in}}^{1-n}|\Delta p_{av}|^{n-1} \quad (6)$$

The average air density in the channel ρ_{cav} is evaluated based on the average air temperature in the solar chimney T_{fav}. A thermal resistance network model based on heat balances of each element of a solar chimney is used to predict the temperature of the air in the chimney as stated in equations (7-9). The thermal model used by Ong & Chow (2003) is adapted with a modification on the heat transfer coefficient prediction in the channel using a correlation found by La Pica et al (1993).

The heat balance at each node for elemental length Dl (figure 3a) results in:

$\mathrm{T_g}$ (Glass): $\mathrm{S_1} + \mathrm{h_{rabg}}(\mathrm{T_{ab}} - \mathrm{T_g}) + \mathrm{h_g}(\mathrm{T_f} - \mathrm{T_g}) = \mathrm{U_g}(\mathrm{T_g} - \mathrm{T_a})$ (7)

$\mathrm{T_f}$ (Air): $\mathrm{h_{ab}}(\mathrm{T_{ab}} - \mathrm{T_f}) = \mathrm{h_g}(\mathrm{T_f} - \mathrm{T_g}) + \dot{q}''$ (8)

$\mathrm{T_{ab}}$ (Absorber) : $\mathrm{S_2} = \mathrm{h_{ab}}(\mathrm{T_{ab}} - \mathrm{T_f}) + \mathrm{h_{rabg}}(\mathrm{T_{ab}} - \mathrm{T_g}) + \mathrm{U_b}(\mathrm{T_{ab}} - \mathrm{T_a})$ (9)

Where $\mathrm{T_g}$, $\mathrm{T_f}$ and $\mathrm{T_{ab}}$ are temperatures of glass, air and absorber for the elemental length respectively. $\mathrm{T_a}$ is the outside air temperature. $\mathrm{S_1}$ & $\mathrm{S_2}$ are absorbed solar radiation by the glass, and the absorber respectively. $\mathrm{h_{rabg}}$ is heat transfer coefficient between the absorber and glass. $\mathrm{h_g}$ is the heat transfer coefficient between air and glass. $\mathrm{U_g}$ is heat transfer coefficient from glass to atmospheric air. $\dot{q}''$is the useful heat gain by the air flowing past the elemental length. U_b is convective heat transfer coefficient from the back insulation. $\mathrm{h_{ab}}$ is the heat transfer coefficient between air and absorber plate.

Equations 7-9 are simultaneously solved to predict the air temperature $\mathrm{T_f}$ for each elemental length and will be averaged out over the chimney length to get T_{fav} . The detailed solution procedure is available in Ong & Chow (2003).

Mass flow rate and temperature prediction in wind induced EAT

EATs make use of the ground as a heat sink and are effective when combined with other passive techniques (Santamouris 2007).

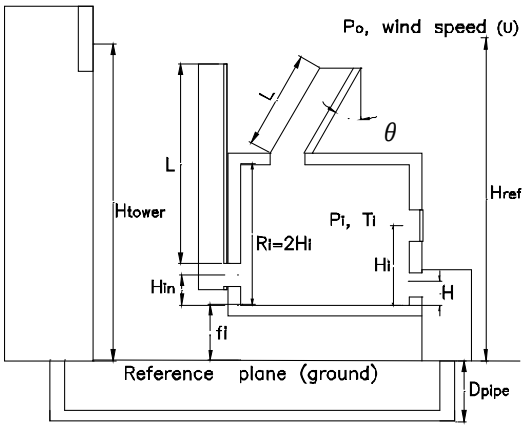

Figure 2 A zone connected to roof mounted solar chimney; wall mounted solar chimney and wind driven earth air tunnel

The major energy consuming element in these systems is a fan whereas their COP is usually more than 10 unlike conventional air conditioning systems with COP around 3 (Goswami, DY & Biseli 1993) except for hot and humid areas . Still the use of a fan can be minimized by capturing wind and tunnelling air into EAT. There is little information on models for wind induced airflow in the EAT. However this configuration has proved to work, as shown for example in a project for an office building in Rome, a building at the university of Cyprus (Allard & Santamouris 1998) and on Sohrabji Godrej green business centre in Hyderabad, India (2004). The present paper discusses a simplified model based on Bernoulli's principle to predict the mass flow rate in the tunnel taking into account both buoyancy and wind in addition to the building pressure distribution.
The available pressure Δp_{av} between inlet and outlet of EAT (figure 2) can be derived using Bernoulli's principle. le.

$$\Delta p_{av} = \frac{\rho_a C p U^2}{2} + \rho_a g(H_{ref} - H_{tower}) + \rho_a g(H_{tower} + Dpip)$$
$$-\rho_{aout} g(H + f_i + Dpip) - (p_i + g\rho_i(H_i - H)) \quad (10)$$

Where H_{tower} is the height of inlet opening of windrower. Dpip is the depth of buried EAT pipe. ρ_{aout} is the air density at the outlet of EAT pipes.
H is height of opening in the connected zone from the floor. It is assumed that the temperature in the wind tower is the ambient temperature (if there is no cooling in the wind tower). ρ_{aout} is evaluated based on the outlet air temperature $T_{air(L)}$ from the EAT (equation 11).
The system flow coefficient C_{syst} for the EAT can be expressed in a similar way as in equation (4)
Local pressure losses at inlet and outlet, due to change in direction, bends, and friction in the EAT can be calculated in a similar approach as used in solar chimneys (Syrios & Hunt 2004) .
A semi analytical thermal resistance model is used to predict the outlet air temperature $T_{air(L)}$ in EAT with the following assumptions. The soil around the pipe is assumed homogenous and the pipe surface temperature is uniform in the axial direction. The soil's undisturbed temperature is taken at the depth of the pipe and a steady state heat transfer is considered at each time step. The model is schematically represented in figure 3b.
The surface temperature at the soil-pipe interface is predicted using the integral method for transient heat conduction in a cylindrical shell subjected to a uniform heat flux at the surface (Necati Ozisik 1980; Goswami, D & Dhaliwal 1985). This effect takes into account the heating up effect of the soil during operation. A similar thermal resistance model is implemented in energy plus (Lee & Strand 2006). However, similar to other simplified models (Tzaferis et al. 1992), the model considers an assumed constant soil thickness and does not account for the transient heating up effect of the soil pipe interface during operation.
The heat transfer in the EAT for an elemental pipe length dx (figure 3b) will be

$$dx[T_{airx} - T_{sur}]/_{R_T} = -\dot{m}c[dT_{air}]; \quad (11)$$

$R_T = R_{pipe} + R_{air}$ $(°C\frac{m}{W})$;
$R_{air} = 1/2\pi r_{pipe} h_{air}$
$R_{pipe} = (1/2\pi k_{pipe})\ln((r_{pipe} + t_{pipe})/r_{pipe})$
Where: R_T overall thermal resistance between air and soil-pipe interface
T_{sur} is temperature at soil-pipe interface
c is specific heat capacity of air
r_{pipe} is inside radius of EAT pipe
t_{pipe} is the thickness of the EAT pipe k_{pipe} is thermal conductivity of the EAT pipe
The outlet air temperature from the EAT $T_{air(x=L)}$ is analytically solved under a boundary condition of $T_{air(x=0)} = T_{amb}$.
T_{sur} is predicted using the integral method .

$$T_{sur} = T_{und} - \frac{q\delta(t)}{k_{soil}} \frac{\ln(1+\frac{\delta(t)}{b})}{\frac{\delta(t)}{b}+2\ln(1+\frac{\delta(t)}{b})} \quad (12)$$

The thermal layer thickness $\delta(t)$ is implicitly expressed as

$$\frac{\alpha_{soil} t}{b^2} = -\frac{(72\eta^2-96\eta+36)\ln\eta - 13\eta + 36\eta - 32\eta + 9}{144(\eta-1)(2ln\,\eta+\eta-1)}$$

Where $\eta = 1 + \delta(t)/b$;
$b = r_{pipe} + t_{pipe}$
$q = -\frac{\dot{m}c}{2\pi r_{pipe} L}(T_{air(L)} - T_{amb})$
k_{soil} is thermal conductivity of the soil
α_{soil} is thermal diffusivity of the soil
t is the elapsed operation time (s)
T_{amb} is outside air temperature
q is heat flux from air in the pipe (W/m^2)
$\delta(t)$ is numerically solved and substituted in equation 12 to find T_{sur} every hour.

a)

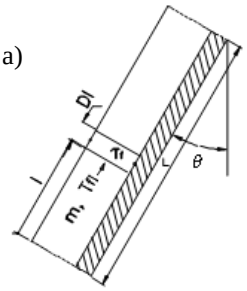

b)

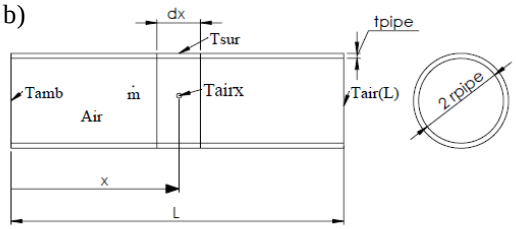

Figure 3 a) control volume of tilted solar chimney; b) pipe element and boundaries considered for EAT thermal model

Building thermal model

The ventilation model should ideally be integrated into the convectional building thermal model. The thermal model currently used is however, a quasi-steady model applied to a lightweight structure. The internal heat load, solar load and the heat transfer through walls, windows, roof, ground and openings are considered in the calculation.
The sensible cooling or heating load to maintain the zone at a specified temperature can be calculated as

$$Q_{load} = \sum_{window} Q_i + \sum_{ventilation\ opening} Q_i + \sum_{internal\ wall} Q_i + \sum_{external\ wall} Q_i + \sum_{light,people\ equipment} Q_i \quad (14)$$

The zone temperature is iteratively predicted from the steady energy balance equation;

$$\sum_{window} Q_i + \sum_{ventilation\ opening} Q_i + \sum_{internal\ wall} Q_i + \sum_{external\ wall} Q_i + \sum_{light,people\ equipment} Q_i = 0 \quad (15)$$

Where Q_i represents the heat transfer into the zone from Windows; external and internal wall; light, people and equipment; or ventilation openings including infiltration.

VALIDATION

Coupled thermal and ventilation model

The output of the present model was compared with well validated TRNSYS-COMIS software for a naturally ventilated single zone building with low are 5mx5mx3m. Other information is stated in Table 1. A simulation was conducted for the first day of January under Adelaide weather condition. The Adelaide data from TRNSYS weather database was taken (figures 4&5).

Table 1
Details of modelled space

External walls	R_{value}=2, north wall is completely shaded
Roof	Metal deck, Rvalue=3.5,ε=0.8,
Windows	On north side, 40% of wall area, U_{value}=2.83, SHGF=0.53, fully shaded externally on south side, 40% of wall area, U_{value}=2.83, SHGF=0.53
Internal heat gain	Full time occupancy. 65W (sensible heat) for each person 2 persons, lighting 5W/m^2, 10.4 W/m^2 computer and other equipment load.
Ventilation opening	Low level opening (north) : 0.6m (height), 2m (width), the lowest level is 0.5m from the ground High level opening (south) : 0.6m (height), 2m (width), the lowest level is 2m from the ground.

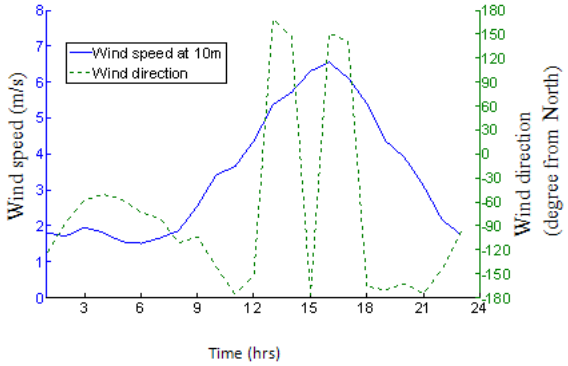

Figure 4 Wind speed and direction considered for the simulation

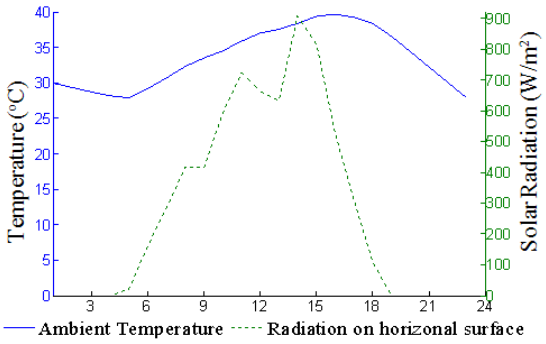

Figure 5 Outside air temperature and global solar radiation on horizontal surface considered for the simulation

The air mass flow rate and sensible cooling loads predicted by both models are presented in figure 6. The maximum percentage error for the cooling load is about 20%. This error is due to the over simplification of the thermal model for the present

study. The maximum percentage error for ventilation prediction is under 4%. Hence, the present model accurately predicts natural ventilation in large openings and can effectively be used to include and compare integrated passive systems.

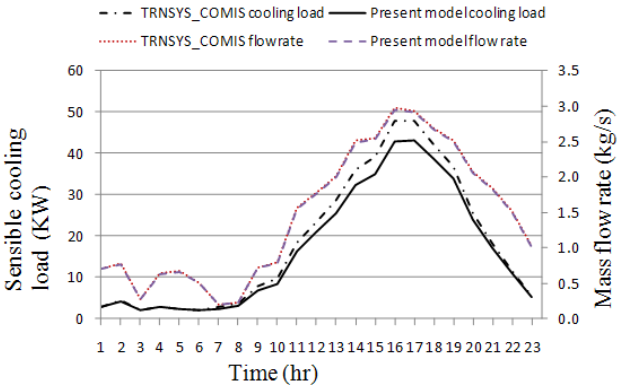

Figure 6 Comparison between TRNSYS-COMIS and Present model for large openings

Solar Chimney

The prediction of mass flow rate in the vertical chimney was compared with Bansal et al.(1993), for Cd=0.6 with varying incident solar radiation. Figure 7 shows the difference is marginal (less than 2%). The comparison between experimental and analytical result of Ong and Chow (2003) with the present model for wall sided vertical chimney (figure 8), shows that the fluid and absorber temperatures are well predicted by the present model for the range of gap depths with respect to the experimental findings and show a closer correlation than the model developed by Ong and Chow (2003).

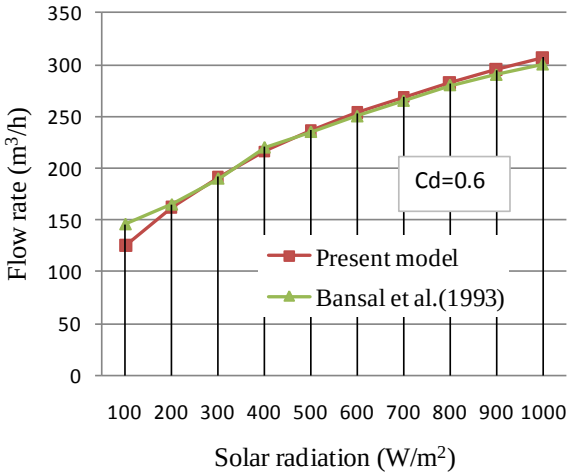

Figure 7 Air flow rate prediction comparison in a roof mounted solar chimney ,comparison with the analytical model of Bansal et al. (1993)

Convergence issue with the solar chimney

The solar chimney model enables us to predict the possibility of reverse air flow to the room. i.e there is

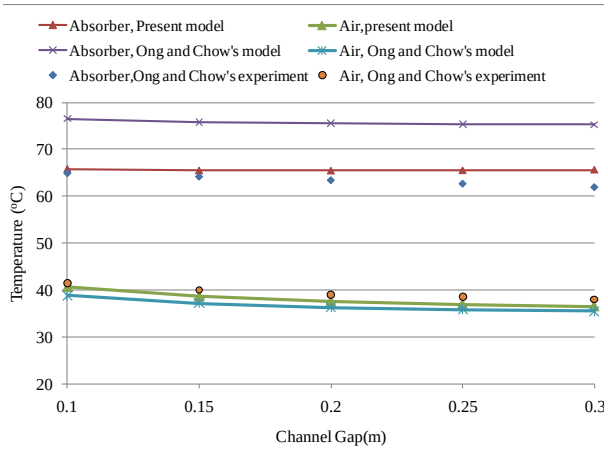

Figure 8 Temperature prediction in solar chimney: comparison with experimental and analytical result of Ong and Chow (2003)

a critical zone pressure (p_i) about which the air flow direction changes. The effect of buoyancy in the chimney is very significant near to this critical pressure and determines the direction of the airflow (equation 3 & 4). If the room temperature is different from the outside air temperature, there is a possibility of recursive chimney temperature T_{fav} as the airflow direction changes during successive iterations. The model will be unstable and convergence will not reach. To avoid this problem, a relaxation factor (F) is applied to the chimney temperature T_{fav} and the corresponding absorber and glass temperature to dampen the oscillation. It is a similar approach taken into TRNFLOW (Weber et al. 2003) to dampen the zone oscillation temperature.

$$T = T_{prev} + F(T - T_{prev}) \qquad (16)$$

Where T represents the air temperature in the chimney, or absorber or glass temperature, and T_{prev} is the temperature in the previous iteration.

F starts with 1 and F = 0.5F if there is recursive temperature during three successive iterations.

The solar chimney property in experimental setup of Ong & Chow (2003) is used to show the effect of the relaxation factor. The air mass flow rate in the solar chimney is predicted for different zone pressures with and without relaxation factor. A room temperature of 25°C; ambient temperature of 27°C; and 200W/m^2 incident radiation on the collector are assumed. Figure 9 shows that the relaxation factor improves the convergence around the critical region and results in the smooth airflow rate curve.

Earth air tunnel (EAT)

The temperature prediction in EAT is compared with experimental findings of Goswami and Dhaliwal (1985). A corrugated plastic pipe of 0.3m diameter and 25m length was buried at 2.1m depth. The experiment was run for 24 hours with a constant air flow rate of 0.0107kg/s. However the data for some hours are not reported.

a)

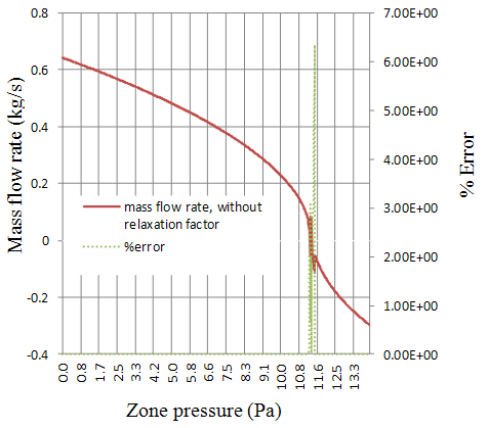

b)

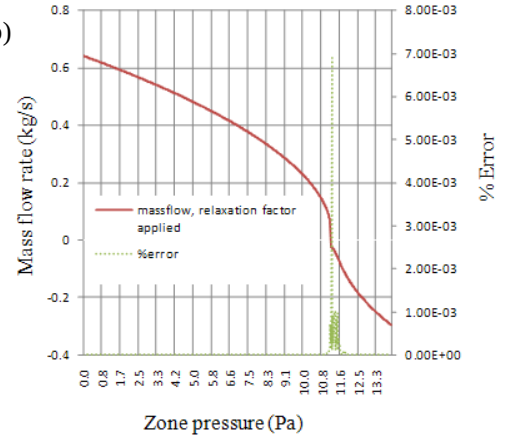

Figure 9 Convergence in solar chimney a) without relaxation factor; b) with relaxation factor

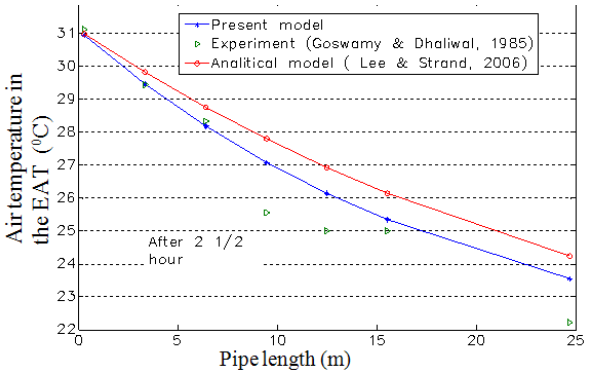

Figure 10 EAT thermal prediction comparison with experimental data of Goswami and Dhaliwal (1985) and analytical model of Lee and Strand (2006).

It was difficult to compare the results for the whole period as some hours data are missing to predict the heating up effect of the pipe-soil interface. The first 2 ½ hrs data was taken from the experiment and the outlet temperature is compared to the present model and a model used by Lee and Strand (2006) . The present model shows a closer correlation than Lee & Strand's model which assumed constant soil thickness equal to the radius of the pipe (figure 10). The error for useful heat transfer rate compared to the experiment is less than 11% for the whole period. It is also suspected that some error with the experimental data might also contribute to the percentage error presented.

APPLICATION OF THE MODEL

The same room used for thermal validation is used with two modifications. A 2m (high) x 2m (width) x 0.3m (gap) vertical solar chimney is laid on the roof of the space (properties for the solar chimney are taken from Ong and Chow (2003). The wind pressure coefficient at the chimney outlet is assumed the value at the roof level (Cp= -0.6).

A wind induced air-earth tunnel is connected through an opening at low level to the room (H_{in}=0.5m high from the floor). A 25m long 0.5m diameter polyethylene pipe is buried at 2m depth. The inlet to the buried pipe is connected to a wind tower. The inlet opening to the wind tower is at 4 m height from the ground. It is assumed that the opening is always facing the windward direction. A sandy-clay soil with thermal conductivity of 1.3 W/m.k and thermal diffusivity of 0.75x10-7 m^2/s is assumed.

Four configurations are tested

1. Low level windows and Solar chimney fully open, Earth-air tunnel and high level windows closed
2. Windows closed, Solar chimney and Earth-air tunnel are fully open
3. All windows and Solar chimney are fully open, and Earth-air tunnel closed
4. All openings are fully open

A constant infiltration of 0.2 (1/hr) is assumed to account for flow through cracks in the zone.

The results show that, the model is able to predict the temperature and the airflow rate in the passive components in case of multi-opening and infiltration as shown in figures 11and12. The chimney model is able to predict the reverse airflow at some hours as shown in configuration 1 (figure 11). The result from the second configuration shows that the combined passive systems may provide significant amount of pre-cooled airflow to the space (figure 11). The variation of airflow characteristics of the solar chimney in configuration 1-4 indicates that any opening in the connected zone may affect the airflow rate in the solar chimney (figures 11&12). In general, this simple example demonstrates that such a model enables designers to investigate the suitability of different configurations of passive airflow components along with a conventional ventilation system.

CONCLUSION

Passive airflow components, which require simultaneous prediction of air temperature and airflow rate, are integrated into the coupled building ventilation and thermal model.

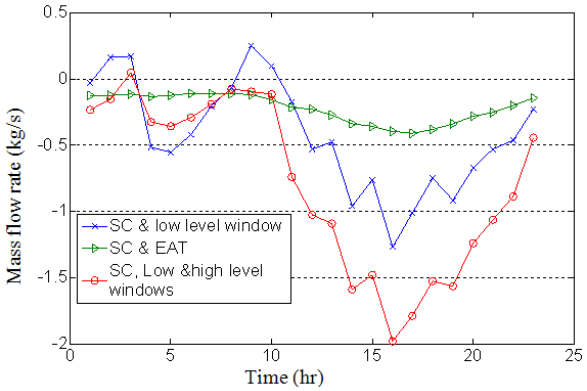

Figure 11 Airflow rate in solar chimney for configurations 1 -3

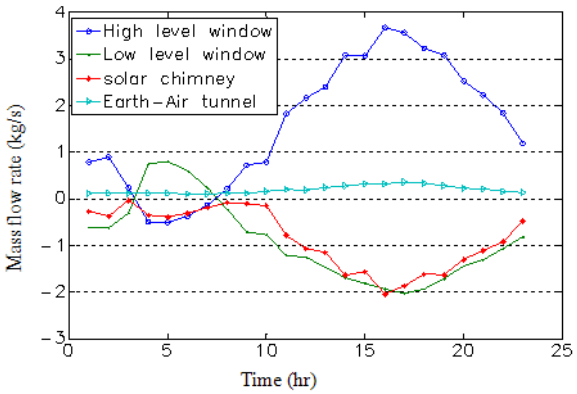

Figure 12 Airflow rate in different openings for configuration 4

This model allows assessment of passive features such as solar chimney and wind induced earth-air tunnel for both natural and hybrid ventilation systems at the design stage. This model is capable of investigating and optimising the design of buildings with passive cooling features.

REFERENCE

Allard, F & Santamouris, M 1998, Natural ventilation in buildings: a design handbook, Earthscan/James & James.

Bahadori, MN, Mazidi, M & Dehghani, AR 2008, 'Experimental investigation of new designs of wind towers, Renewable Energy', vol. 33, no. 10, pp. 2273-2281.

Bansal, NK, Mathur, R & Bhandari, MS 1993, 'Solar chimney for enhanced stack ventilation', Building and Environment, vol. 28, no. 3, pp. 373-377.

Bansal, NK, Mathur, R & Bhandari, MS 1994, 'A study of solar chimney assisted wind tower system for natural ventilation in buildings', Building and Environment, vol. 29, no. 4, pp. 495-500.

Bassiouny, R & Koura, NSA 2008, 'An analytical and numerical study of solar chimney use for room natural ventilation', Energy and Buildings, vol. 40, no. 5, pp. 865-873.

Chen, Q 2009, 'Ventilation performance prediction for buildings: A method overview and recent applications', Building and Environment, vol. 44, no. 4, pp. 848-858.

Dennis, J & Schnabel, R 1996, Numerical methods for unconstrained optimization and nonlinear equations, Society for Industrial Mathematics.

Goswami, D & Dhaliwal, A 1985, 'Heat transfer analysis in environmental control using an underground air tunnel', Journal of Solar Energy Engineering, vol. 107, p. 141.

Goswami, DY & Biseli, KM 1993, Use of Underground Air Tunnels for Heating and Cooling Agricultural and Residential Buildings, University of Florida.

Lee, K & Strand, R 2006, 'Implementation of an earth tube system into Energy Plus program', paper presented at the SimBuild 2006 Conference, Boston MA, USA.

Maerefat, M & Haghighi, AP 2010, 'Passive cooling of buildings by using integrated earth to air heat exchanger and solar chimney', Renewable Energy, vol. 35, no. 10, pp. 2316-2324.

Necati Ozisik, M 1980, 'Heat conduction', North Carolina State Univcrsity, vol. 58.

Ohba, M & Lun, I 2010, 'Overview of natural cross-ventilation studies and the latest simulation design tools used in building ventilation-related research', Advances in Building Energy Research, vol. 4, no. 2, pp. 127-166.

Ong, KS & Chow, CC 2003, 'Performance of a solar chimney', Solar Energy, vol. 74, no. 1, pp. 1-17.

Rediff, T 2004, viewed feb 28 2011, <http://www.solaripedia.com/13/94/814/godrej_green_business_center_wind_tower_(india).html>.

Santamouris, M 2007, Advances in passive cooling, Earthscan.

Syrios, K & Hunt, G 2004, 'Paper 1: Design Considerations for Roof-Mounted Ventilation Systems', International Journal of Ventilation, vol. 3, no. 2.

Tzaferis, A, Liparakis, D, Santamouris, M & Argiriou, A 1992, 'Analysis of the accuracy and sensitivity of eight models to predict the performance of earth-to-air heat exchangers', Energy and Buildings.

Weber, A, Koschenz, M, Dorer, V, Hiller, M & Holst, S 2003, 'TRNFLOW, a new tool for the modelling of heat, air and pollutant transport in buildings within TRNSYS', paper presented at the 8th International IBPSA Conference, Eindhoven, Netherlands.

Zhengen, R & Zhendong, C 2009, 'Enhanced air flow modelling for AccuRate - a nationwide house energy rating tool in Australia', Building and Environment, 12 November.